Semiconductor(BaSi$_2$)/metal(CoSi$_2$) Schottky-barrier structures epitaxially grown on Si(111) substrates by molecular beam epitaxy

Takashi Suemasu[a,b], Masato Sasase[c], Yoshitake Ichikawa[a], Michitaka Kobayashi[a] and Dai Tsukada[a]

[a]*Institute of Applied Physics, University of Tsukuba, 1-1-1 Tennohdai, Tsukuba, Ibaraki*

305-8573, Japan

[b]*PRESTO, Japan Science and Technology Agency, Chiyoda-ku, Tokyo 102-0075, Japan*

[c]*The Wakasa Wan Energy Research Center, Tsuruga, Fukui 914-0192*, Japan

Corresponding author: Takashi Suemasu

Institute of Applied Physics, University of Tsukuba, Tsukuba, Ibaraki 305-8573, Japan

TEL/FAX: +81-29-853-5111, Email: suemasu@bk.tsukuba.ac.jp

We successfully demonstrated epitaxial growth of semiconductor(BaSi$_2$)/metal(CoSi$_2$)

Schottky-barrier structures on Si(111), for the first time, by molecular beam epitaxy (MBE).

The interface between the CoSi$_2$ and BaSi$_2$ layers was found to be sharp, from transmission

electron microscopy (TEM) observations. The current-voltage characteristics measured at room temperature showed clear rectifying properties. When positive bias was applied to the $CoSi_2$ layer with respect to the $BaSi_2$ layer, the current increased exponentially. Electron diffraction patterns obtained using reflection high-energy electron diffraction (RHEED) and TEM are discussed.

1. Introduction

Semiconducting silicides, such as β-FeSi$_2$ and BaSi$_2$, have attracted significant recent attention as Si-based new materials. There have been a number of reports on infrared light-emitting diodes and detectors using β-FeSi$_2$ [1-4]. In contrast, there have been very few reports on BaSi$_2$. BaSi$_2$ has a very large optical absorption coefficient of over 10^5 cm^{-1} at 1.5 eV [5,6]. This value is approximately two orders of magnitude larger than that of Si, and has been attributed to large values of dipole matrix elements across the gap due to a mixture of Ba-pd and Si-spd states [6]. In addition, the band gap of BaSi$_2$ was found to reach the ideal value of approximately 1.4 eV matching the solar spectrum by replacing half of the Ba atoms with isoelectric Sr atoms [7-11]. We therefore believe that BaSi$_2$ is very promising as a material for high-efficiency thin-film solar cells.

Our research is aimed at realizing CoSi$_2$/n-Ba$_{1-x}$Sr$_x$Si$_2$ Schottky-barrier solar cells. CoSi$_2$ is a metallic silicide with a lattice constant of 0.536 nm, which almost matches the lattice constant of Si (0.543 nm). Semiconducting BaSi$_2$ has an orthorhombic structure (BaSi$_2$-type structure, space group $Pnma$) at atmospheric pressure and room temperature (RT) with lattice constants a=0.891 nm, b=0.672 nm, c=1.153 nm [12-14]. In addition, BaSi$_2$ has a small electron affinity of approximately 3.3 eV [15], and CoSi$_2$ has a work function of approximately 4.7 eV [16]. Undoped BaSi$_2$ usually shows n-type conductivity with a small

electron concentration of approximately 10^{16}cm^{-3} [5,17]. Thus, a Schottky-barrier (SB) height

as large as 1.4 eV is expected for the CoSi$_2$/n-Ba$_{1-x}$Sr$_x$Si$_2$ interface. This large barrier height

reduces the saturation current density, resulting in a large open-circuit voltage in the SB solar

cells [18]. Furthermore, photogenerated carriers are efficiently collected before recombination

due to a large built-in potential throughout the optical absorption layers of n-Ba$_{1-x}$Sr$_x$Si$_2$. We

have developed an epitaxial growth technique for BaSi$_2$ and Ba$_{1-x}$Sr$_x$Si$_2$ films on Si(111)

substrates using molecular beam epitaxy (MBE) [19-22]. The epitaxial growth of

Si/CoSi$_2$/Si(111) structures has also been reported [23,24]. However, there have been no

reports thus far on the formation of BaSi$_2$/CoSi$_2$ hybrid structures. The purpose of this study is

to form BaSi$_2$/CoSi$_2$ hybrid structures on Si(111) by MBE, and to confirm the rectifying

properties of their current-voltage (*I-V*) characteristics as a first step towards realizing the

BaSi$_2$/CoSi$_2$ SB solar cells.

2. Experimental

BaSi$_2$/CoSi$_2$ hybrid structures were epitaxially grown on Si(111) using an

ion-pumped MBE system equipped with Knudsen cells for Ba and Co, and an electron-beam

4

evaporation source for Si. After cleaning the Si(111) wafers thermally in ultrahigh vacuum (UHV), Co was first evaporated on to Si(111) at RT, followed by 690ºC annealing to form 27-nm-thick $CoSi_2$ layers by solid phase epitaxy (SPE; Co deposition at RT, followed by high-temperature annealing). The thickness of a $CoSi_2$ film was calculated using the theoretical densities of Co, Si and $CoSi_2$; 1 nm of Co results in 3.46 nm of $CoSi_2$. Then, 10-nm-thick Si was epitaxially grown on the $CoSi_2$ layers at 590ºC; this Si layer was transformed into approximately 22-nm-thick $BaSi_2$ films by reaction deposition epitaxy (RDE; Ba deposition on hot Si) [19,25]. The $BaSi_2$ thin films were used as a template to control the crystal orientation of the $BaSi_2$ overlayers [20]. Finally, Si and Ba were coevaporated on the $BaSi_2$ template to form $BaSi_2$ by MBE. The total thickness of the $BaSi_2$ layers was approximately 240 nm. For reference, two other samples, approximately 200-nm-thick $BaSi_2$ and 40-nm-thick $CoSi_2$ films epitaxially grown on the Si(111) substrates were prepared. The deposition rates of Ba and Si were controlled using a quartz crystal monitor.

The crystal quality of the $BaSi_2$ and $CoSi_2$ thin films was characterized by reflection high-energy electron diffraction (RHEED) and θ–2θ X-ray diffraction (XRD). High-resolution cross-sectional observations were performed by transmission electron microscopy (TEM; JEOL, JEM-3000F). The acceleration voltage was maintained at 300 kV. RHEED and TEM observations were performed along the [11-2] azimuth of Si. Thin foils for

5

TEM observation were prepared with a focused ion beam (FIB) micro-sampling system. Dimensions of the FIB fabricated part were approximately 15 ×15×1 μm^3. These parts were removed from the specimen and fixed on a Cu mesh. Pt was deposited on the sample surface to reduce damage at the time of specimen fabrication in the region for observation. For *I-V* characteristics of the SB structure, a 1-mm^2 mesa structure was fabricated by wet chemical etching. Ohmic contacts were formed on the *n*-BaSi$_2$ and CoSi$_2$ layers.

3. Results and discussion

3.1 Epitaxial growth of BaSi$_2$/CoSi$_2$ layers on Si(111)

Figure 1(a-d) shows RHEED patterns taken along the [11-2] azimuth of Si after the formation of (a) CoSi$_2$, (b) Si, (c) BaSi$_2$ template and (d) MBE-grown BaSi$_2$ layers. Streaky patterns were obtained at every growth stage. It can be seen in Figs. 1(c) and 1(d) that the streaks of BaSi$_2$ appear, dividing the spacing of 1×1 Si streaks (lines) into approximately six equal intervals. In Fig. 2, the θ-2θ XRD pattern shows that only the diffraction peaks of (100)-oriented BaSi$_2$, such as (200), (400) and (600) of BaSi$_2$, and (111)-oriented CoSi$_2$ were observed. On the basis of these results, we conclude that the BaSi$_2$/CoSi$_2$ hybrid structures were epitaxially grown on Si(111). This is the first epitaxial heterostructures of metallic silicide and semiconducting silicide. The forbidden diffraction peak of Si(222) occurs by double diffraction.

In SB solar cells, the $BaSi_2/CoSi_2$ interface is very important. In order to investigate the $BaSi_2/CoSi_2$ interface, TEM observations were carried out. Figures 3(a) and 3(b) show cross-sectional TEM images taken at low and high magnifications, respectively. It was confirmed that the $BaSi_2/CoSi_2$ hybrid structure was formed, and that the $BaSi_2/CoSi_2$ interface was sharp. The grain size of $BaSi_2$ is estimated to be approximately 0.2 μm from the contrast in the TEM image. Figure 3(c) shows the transmission electron diffraction (TED) pattern taken in an area including the $BaSi_2$, $CoSi_2$ and Si as indicated by the circle in Fig. 3(a). This diffraction pattern consists of diffraction spots of $BaSi_2$, $CoSi_2$ and Si. We can see 4×7 diffraction spots of $BaSi_2$ in a rectangle composed of (000) and, (111), (31-1) and (20-2) diffraction spots of Si and $CoSi_2$. The diffraction positions of $CoSi_2$ and Si are almost the same. Figures 4(a) and 4(b) show the cross-sectional TEM image and the TED pattern of the $CoSi_2/Si(111)$ interface, respectively. We can see that the diffraction spots such as (111), (31-1) and (20-2) of $CoSi_2$ almost overlap with those of Si. The origin of the diffraction pattern shown in Fig. 3(c) is discussed later.

Figure 5 shows the *I-V* characteristics measured at RT. The undoped $BaSi_2$ shows *n*-type conductivity [5,17]. The current increased exponentially when positive bias was applied to the $CoSi_2$ layer with respect to the *n*-$BaSi_2$ layer, showing that the SB structure was formed.

3.2 Electron diffraction patterns of BaSi₂/CoSi₂/Si

The crystal orientation of the BaSi$_2$ layer formed on the CoSi$_2$ is thought to be the same as that formed directly on the Si(111) substrates. This is because the BaSi$_2$ layer was grown on the (111)-oriented Si epitaxial layer formed on the CoSi$_2$/Si(111) in this work. It was found from X-ray pole-figure measurements that the *a*-axis-oriented BaSi$_2$ epitaxial layers on Si(111) have three distinct but crystallographically equivalent epitaxial variants rotated with respect to each other by 120º in the surface normal direction as shown in Fig. 6 [20]. The three-fold symmetry of BaSi$_2$ on Si(111) is thought to be due to the three-fold symmetry of the Si(111) surface. Figure 7 shows the θ-2θ XRD pattern of BaSi$_2$ epitaxial layers on Si(111). The diffraction peaks of only (100)-oriented BaSi$_2$, such as (200), (400) and (600) of BaSi$_2$, are observed. Figure 8 shows the (a) TEM cross-sectional image at the BaSi$_2$/Si(111) interface and (b) the TED pattern observed along the Si[11-2]. The TED pattern shown in Fig. 8(b) is identical to that shown in Fig. 3(c), indicating that the crystal orientation of the BaSi$_2$ layer on CoSi$_2$ is the same as that formed directly on Si(111).

The TED patterns, shown in Fig. 8(b), consist of those of Si and BaSi$_2$. There are three kinds of epitaxial variants of BaSi$_2$ denoted as A, B and C as shown in Fig. 6. Among these, the diffraction pattern of type-A BaSi$_2$ is expected to be the same as that of type-C BaSi$_2$ when the electron beam is incident along Si[11-2]; however, it is different from that of type-B BaSi$_2$. Figures 9 and 10 show the schematic images of theoretically predicted

transmission RHEED patterns of $BaSi_2$ and TED patterns of $BaSi_2/CoSi_2/Si$ structures for type-A and type-B $BaSi_2$, respectively, when the electron beam is incident along Si[11-2]. The diffraction positions of $BaSi_2$, Si and $CoSi_2$ are indicated by ●, □ and △, respectively. In the case of type-A $BaSi_2$, the electron beam was incident along $BaSi_2$[0-11]. The plane spacing of $BaSi_2$(033) (0.194 nm) is almost the same as that of Si{220}. Thus, the diffraction spots of $BaSi_2$ appear on the lines which divide the spacing of 1×1 Si streaks (lines) into almost three equal intervals as shown in Fig. 9(a). In addition, the plane spacing of $BaSi_2$(600) is almost the same as that of $CoSi_2$(222). Therefore, the TED pattern shown in Fig. 9(b) is expected in this case. On the other hand, the electron beam was incident along $BaSi_2$[110] for type-B $BaSi_2$. In this case, the plane spacing of $BaSi_2$(006) (0.193 nm) is almost the same as that of Si{220}. Thus, the diffraction spots of $BaSi_2$ appear on the lines which divide the spacing of 1×1 Si streaks into almost six equal intervals as shown in Fig. 10(a). Therefore, the TED pattern shown in Fig. 10(b) is expected in this case. On the basis of the discussion above, we conclude that the diffraction spots of the three epitaxial variants of $BaSi_2$ on Si(111) appear on the lines dividing the spacing of Si 1×1 streaks into six as shown in Figs. 3(c) and 8(b). The RHEED streaks of $BaSi_2$ shown in Figs. 1(c) and 1(d) agree with this assumption. We think that the three epitaxial variants of $BaSi_2$ are distributed equally as reported in the $BaSi_2$ epitaxial layers on Si(111) [20]. In Figs. 3(c) and 8(b), however, the diffraction spots of $BaSi_2$ corresponding to (100), (300), (500), (001), (003), (005) are also observed. These diffraction

9

spots are theoretically forbidden. Double diffraction could be the origin of these diffraction spots. We have not yet investigated the influence of three epitaxial variants of $BaSi_2$ on the electrical and optical properties of $BaSi_2$. We think that the light is absorbed in the $BaSi_2$ layer of the strong electric field in a $BaSi_2/CoSi_2$ SB structure, resulting in efficient extraction of photogenerated electrons and holes. Thus, useful solar cells can be made in $BaSi_2$ if the $BaSi_2$ films are sufficiently thin and have high absorption coefficient together with requisite mobilities.

4. Conclusions

We have succeeded in growing the $BaSi_2$(240 nm)/$CoSi_2$(27 nm) Schottky-barrier structure epitaxially on Si(111) by MBE. The *I-V* characteristics of the diode showed clear rectifying properties due to the SB structure at RT. TEM observations showed that the $BaSi_2/CoSi_2$ interface was sharp. The streaky RHEED patterns and TED patterns observed could be well explained by *a*-axis-oriented $BaSi_2$ with three equivalent epitaxial variants rotated with respect to each other by 120º in the surface normal direction.

References

[1] D. Leong, M. Harry, K. J. Reeson, K. P. Homewood, Nature **387** (1997) 686.

[2] T. Suemasu, Y. Negishi, K. Takakura, F. Hasegawa, Jpn. J. Appl. Phys. **39** (2000) L1013.

[3] T. Suemasu, Y. Negishi, K. Takakura, F. Hasegawa, Appl. Phys. Lett. **79** (2001) 1804.

[4] T. Ootsuka, Y. Fudamoto, M. Osamura, T. Suemasu, Y. Makita, Y. Nakayama, Y. Fukuzawa, Appl. Phys. Lett. **91** (2007) 142114.

[5] K. Morita, Y. Inomata, T. Suemasu, Thin Solid Films **508** (2006) 363.

[6] D. B. Migas, V. L. Shaposhnikov, V. E. Borisenko, Phys. Stat. Sol. (b) **244** (2007) 2611.

[7] K. Ojima, M. Yoshimura, K. Ueda, Jpn. J. Appl. Phys. **41** (2002) 4965.

[8] K. Morita, Y. Inomata, T. Suemasu, Jpn. J. Appl. Phys. **45** (2006) L390.

[9] K. Morita, M. Kobayashi, T. Suemasu, Thin Solid Films **515** (2007) 8216.

[10] T. Suemasu, K. Morita, M. Kobayashi, J. Cryst. Growth **301-302** (2007) 680.

[11] Y. Imai, A. Watanabe, Thin Solid Films **515** (2007) 8219.

[12] H. Schäfer, K. H. Janzon, A. Weiss, Angew. Chem. Int. Ed. Engl. **2** (1963) 393.

[13] J. Evers, G. Oehlinger, A. Weiss, Angew. Chem. Int. Ed. Engl. **16** (1977) 659.

[14] M. Imai, T. Hirano, T. Kikegawa, O. Shimomura, Phys. Rev. B **55** (1997) 132.

[15] T. Suemasu, K. Morita, M. Kobayashi, M. Saida, M. Sasaki, Jpn. J. Appl. Phys. **45**

(2006) L519.

[16] C. Pirri, J. C. Peruchetti, D. Bolmont, G. Gewinner, Phys. Rev. B **33** (1986) 4108.

[17] T. Nakamura, T. Suemasu, K. Takakura, F. Hasegawa, Appl. Phys. Lett. **81** (2002) 1032.

[18] S. M. Sze, Physics of Semiconductor Devices, John Wiley & Sons, New York, 1981, p.822.

[19] Y. Inomata, T. Nakamura, T. Suemasu, F. Hasegawa, Jpn. J. Appl. Phys. **43** (2004) 4155.

[20] Y. Inomata, T. Suemasu, F. Hasegawa, Jpn. J. Appl. Phys. **43** (2004) L478.

[21] Y. Inomata, T. Suemasu, T. Izawa, F. Hasegawa, Jpn. J. Appl. Phys. **43** (2004) L771.

[22] M. Kobayashi, K. Morita, T. Suemasu, Thin Solid Films **515** (2007) 8242.

[23] R. T. Tung, J. L. Batstone, S. M. Yalisove, J. Electrochem. Soc. **136** (1989) 815.

[24] M. Miyao, K. Nakagawa, N. Nakamura, T. Ohshima, J. Cryst. Growth **111** (1991) 957.

[25] R. A. Mackee, F. J. Walker, J. R. Conner, R. Raj, Appl. Phys. Lett. **63** (1993) 2818.

Figure captions

Figure 1   RHEED patterns taken along Si [11-2] after the growth of (a) $CoSi_2$, (b) Si,

(c) $BaSi_2$ template and (d) MBE-grown $BaSi_2$ layers.

Figure 2 θ-2θ XRD pattern of the $BaSi_2$/$CoSi_2$ structure epitaxially grown on Si(111).

Figure 3   Cross-sectional TEM images of the $BaSi_2$/$CoSi_2$/Si(111) structures observed

at (a) low magnification and (b) high magnification, and (c) TED pattern taken along Si[11-2].

The circle indicates the area of TED observation.

Figure 4   (a) Cross-sectional TEM image of the $CoSi_2$/Si(111) structure and (b) TED

pattern taken along Si[11-2]. The circle indicates the area of TED observation.

Figure 5   Current-voltage characteristics measured at RT.

Figure 6   Schematic model of $BaSi_2$ films epitaxially grown on Si(111). There are

three distinct but crystallographically equivalent epitaxial variants.

Figure 7 θ-2θ XRD pattern of BaSi$_2$ layers epitaxially grown on Si(111).

Figure 8   (a) TEM cross-section of BaSi$_2$ layers on Si(111) and TED pattern taken along Si[11-2]. The area of TED observation is approximately 0.5 μm in diameter around the BaSi$_2$/Si interface.

Figure 9   Schematic images of (a) a transmission RHEED pattern of BaSi$_2$ and (b) a TED pattern of BaSi$_2$/CoSi$_2$/Si for type-A BaSi$_2$. Theoretical diffraction positions of BaSi$_2$, Si and CoSi$_2$ observed along Si[11-2] are indicated as ●, □ and △, respectively. Arrows indicate the positions dividing the spacing of 1×1 Si streaks (lines) into three equal intervals.

Figure 10   Schematic images of (a) a transmission RHEED pattern of BaSi$_2$ and (b) a TED pattern of BaSi$_2$/CoSi$_2$/Si for type-B BaSi$_2$. Theoretical diffraction positions of BaSi$_2$, Si and CoSi$_2$ observed along Si[11-2] are indicated as ●, □ and △, respectively. Arrows indicate the positions dividing the spacing of 1×1 Si streaks (lines) into six equal intervals.
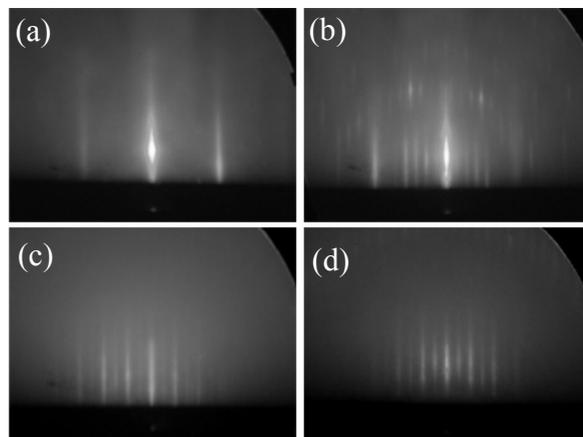
Fig. 1 Suemasu *et al.*

Fig. 2 Suemasu *et al.*

(a) Pt BaSi₂ CoSi₂ Si(111) 0.2 μm

(b) BaSi₂ CoSi₂ 5 nm Si

(c) 111_Si 000 220_Si

Fig. 3 Suemasu *et al.*

(a)

Pt

CoSi$_2$

Si(111)

0.1 μm

(b)

111$_{Si, CoSi_2}$

000　　220$_{Si, CoSi_2}$

Fig. 4 Suemasu *et al*.

0.5 mA/div

5 V/div
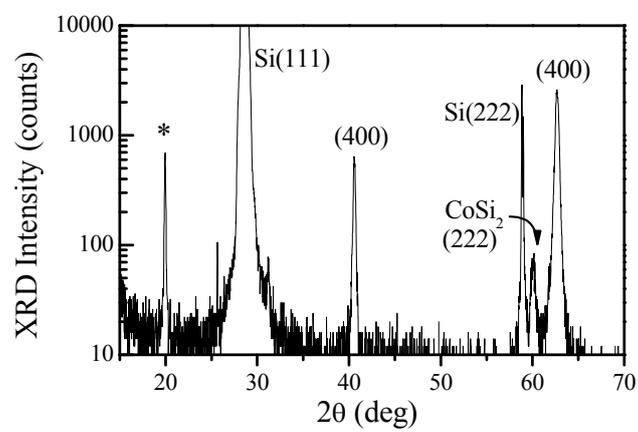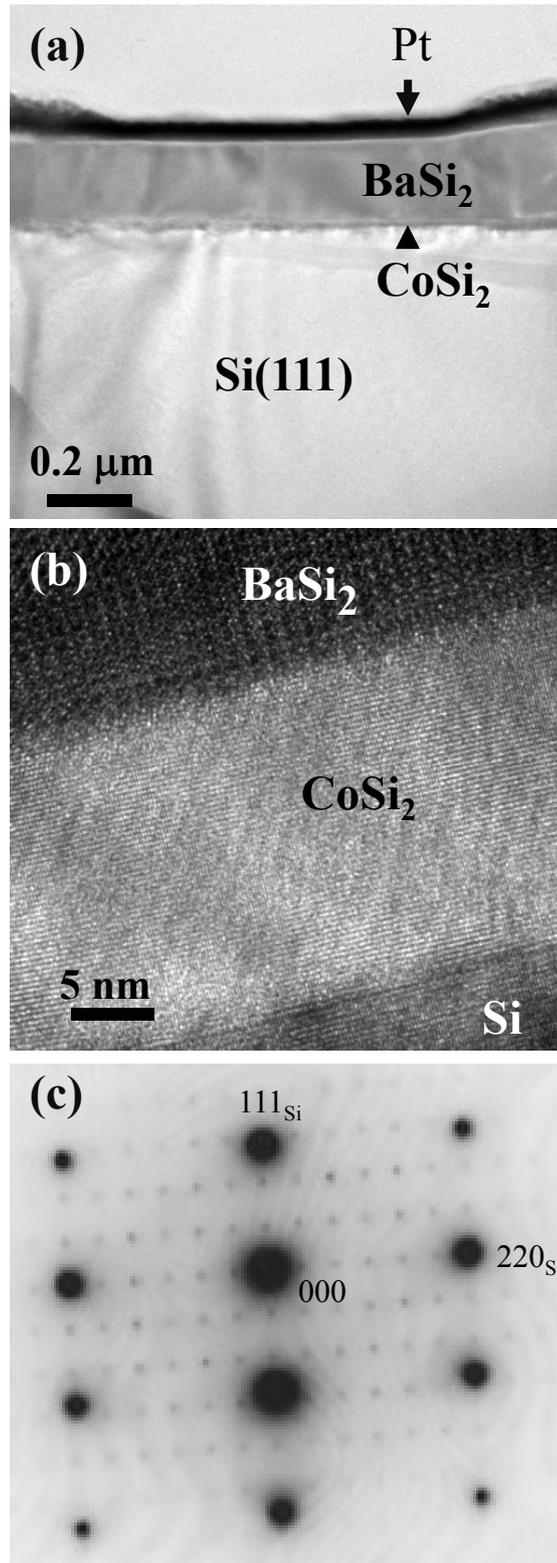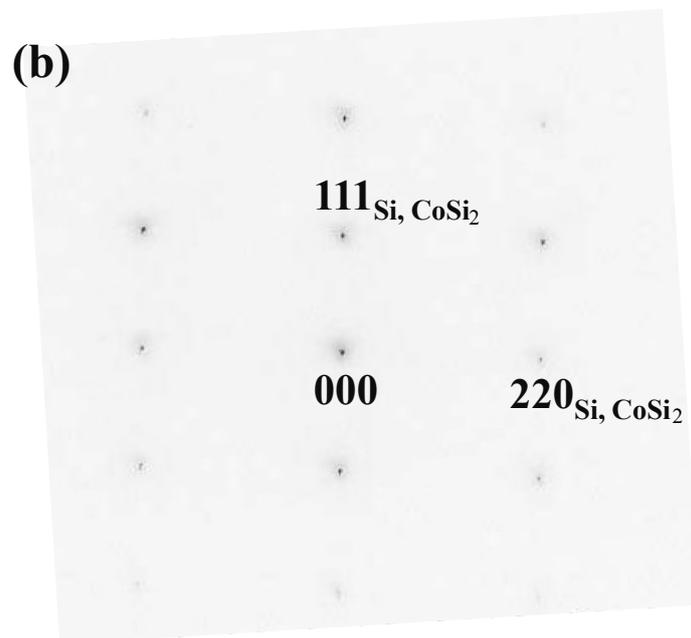
Fig. 5 Suemasu *et al.*
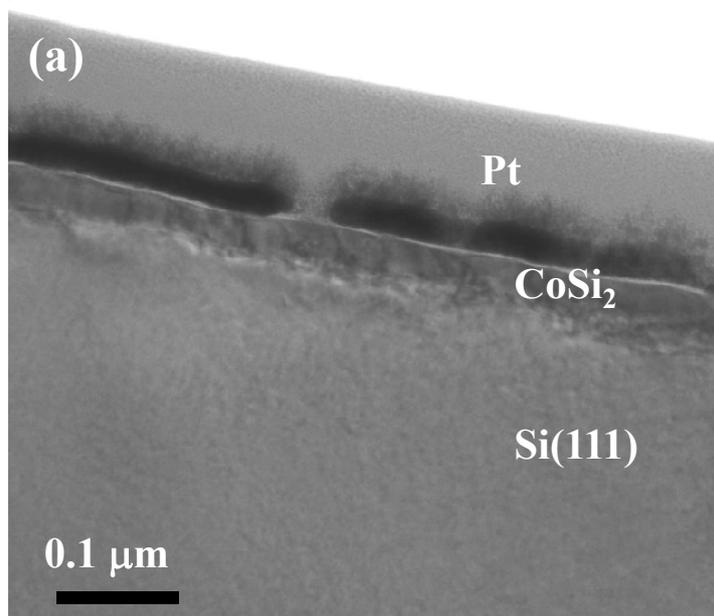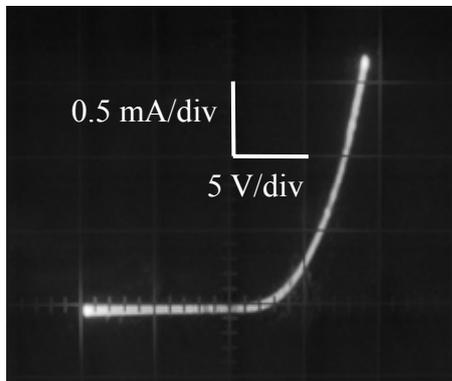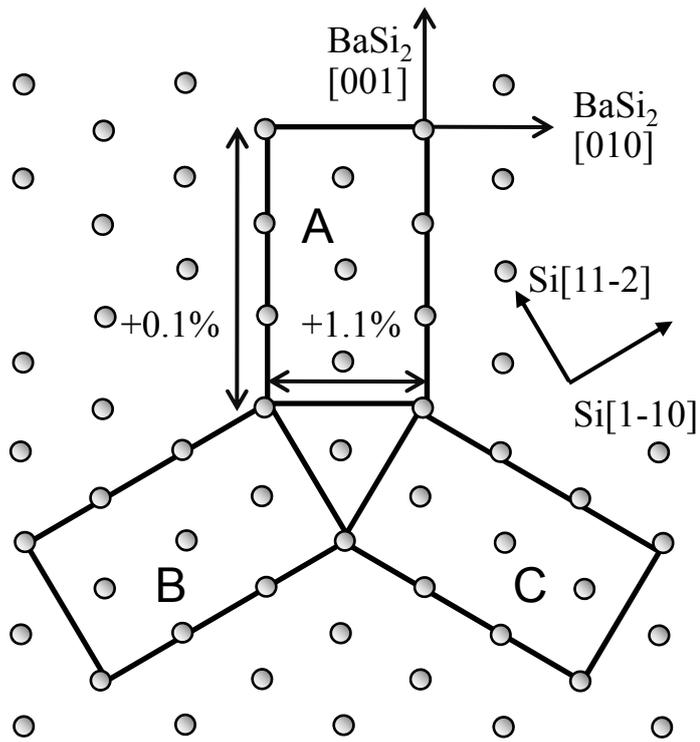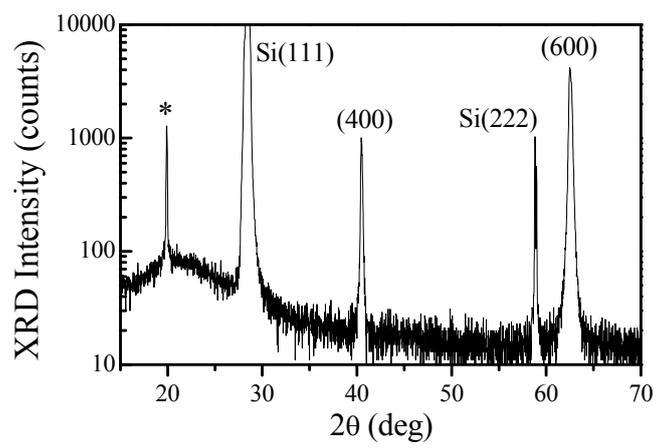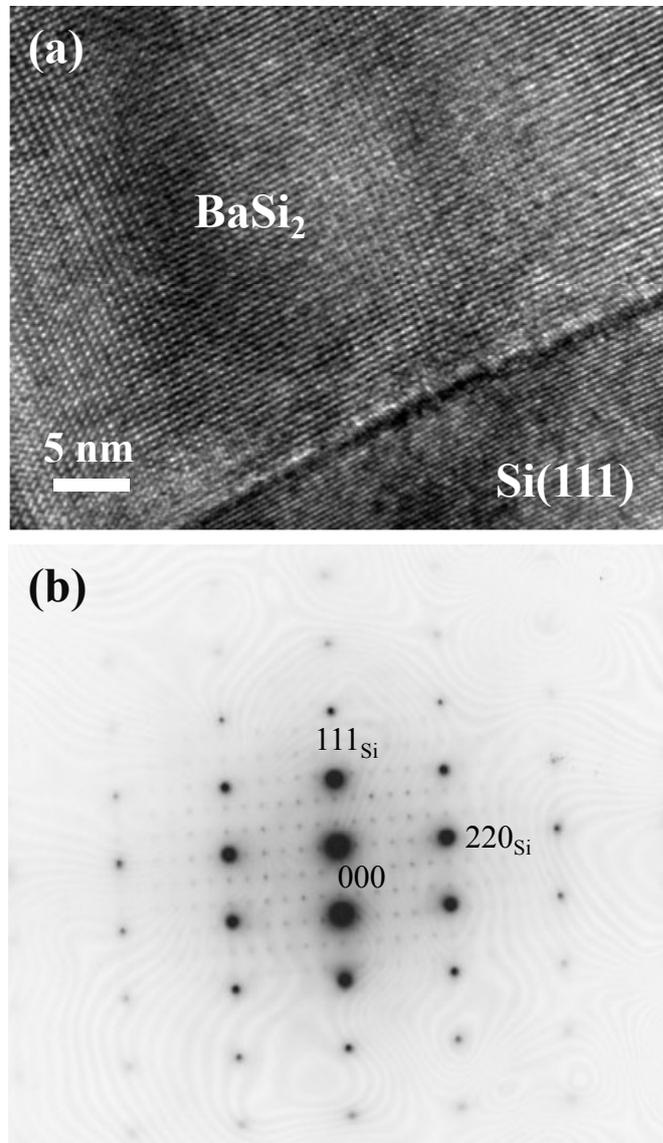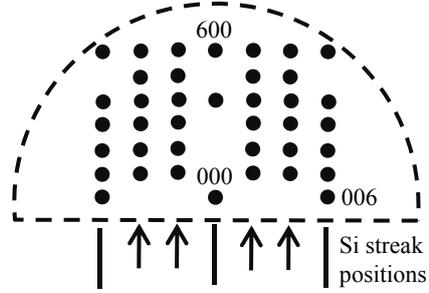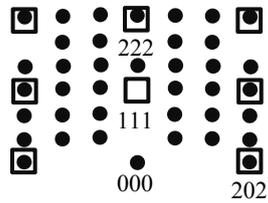
Fig. 6 Suemasu *et al.*

Fig. 7 Suemasu *et al.*

(a) BaSi₂ / 5 nm / Si(111)

(b) 111_Si / 220_Si / 000

Fig. 8 Suemasu *et al.*

(a) Type A

Transmission RHEED of BaSi$_2$ along BaSi$_2$[011]

600

000

006

Si streak
positions

TEM diffraction of BaSi$_2$/(CoSi$_2$)/Si(111)

222

111

000

202

(b) Type B

Transmission RHEED of BaSi$_2$ along BaSi$_2$[010]

600

000

006

Si streak
positions

TEM diffraction of BaSi$_2$/(CoSi$_2$)/Si(111)

000

202
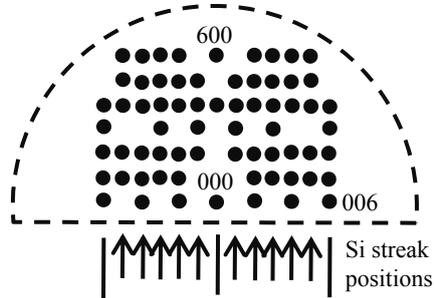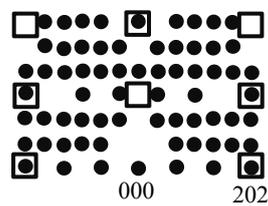
☐ Si(CoSi$_2$) allowed diffraction

Fig. 9 Suemasu *et al.*